Revista Mexicana de Astronomía y Astrofísica, **53**, 235–246 (2017)

OBSERVATIONS AND LIGHT CURVE SOLUTIONS OF SIX DEEP-CONTACT W UMA BINARIES

Diana P. Kjurkchieva[1], Velimir A. Popov[1,2], Doroteya L. Vasileva[1], and Nikola I. Petrov[3]

Received February 20 2017; accepted April 7 2017

ABSTRACT

This work presents photometric observations of the W UMa binaries V0637 Peg. V0473 Cam, CSS J153314.8+560527, CSS J075258.0+382035, V0416 Gem and NSVS 6859986, made using Sloan g' and i' filters. The periods of these binaries are in the range of 0.26–0.43 d. The light curve solutions revealed that the components of each binary system are almost equal in temperature. The stellar components are of G and K spectral types and undergo total eclipses. All observation targets have deep-contact configurations with a fill-out factor of $f \geq 0.5$. NSVS 6859986 has one of the highest fill-out factors that have been determined, $f = 0.84$. We studied the empirical dependencies between the fill-out factor and the stellar parameters (temperature, period, mass ratio, relative component radii, and luminosity ratio) in a sample of around thirty stars; they are consistent with theoretical predictions, although there are deviations from the main tendencies.

RESUMEN

Se presentan observaciones fotométricas de las binarias tipo W UMa V0637 Peg. V0473 Cam, CSS J153314.8+560527, CSS J075258.0+382035, V0416 Gem y NSVS 6859986, con los filtros g' y i' del Sloan. Sus períodos están comprendidos entre 0.26 y 0.46 días. Las soluciones a las curvas de luz revelan que ambas componentes tienen temperaturas casi iguales. Las componentes son de tipos G y K, y presentan eclipses totales. Todos los sistemas tienen configuraciones de contacto profundo, con factores de llenado $f \geq 0.5$. NSVS 6859986 tiene uno de los mayores factores de llenado conocidos, f =0.84. Estudiamos las dependencias empíricas entre el factor de llenado y los parámetros estelares (temperatura, período, cociente de masas, radios relativos de las componentes, y cociente de sus luminosidades) para una muestra de alrededor de 30 estrellas. Encontramos buena concordancia con las predicciones teóricas, pese a algunas desviaciones.

Key Words: binaries: eclipsing — binaries: close — stars: fundamental parameters

1. INTRODUCTION

W UMa type stars are binaries of spectral type F0-K5 whose components have nearly equal surface temperatures and luminosities, despite their often greatly different masses (Binnendijk 1965). The model of Lucy (1968a,b) explained this effect by a common envelope (CE). The orbital motion of the two stellar components inside this envelope makes them lose angular momentum and eventually spiral towards each other (Webbink 1984, Qian 2003, Willems & Kolb 2004, Stepien 2006, Ivanova et al. 2013).

The PLC relationships of W UMa stars, combined with their ease of detection, make these binaries useful distance tracers (Klagyivik & Csizmadia 2004, Gettel et al. 2006, Eker et al. 2008). But the more important aspect of W UMa stars for modern astrophysics is that they provide information about the processes that drive tidal interactions, mass loss and mass transfer, angular momentum loss, and the merging of stars (Martin et al. 2011). Stellar merg-

[1]Department of Physics, Shumen University.
[2]IRIDA Observatory, Rozhen NAO, Bulgaria.
[3]Institute of Astronomy and NAO, Bulgarian Academy of Sciences.

ers have been considered as a plausible origin of stellar eruptions of the V838 Mon (Munari et al. 2002) and V1309 Sco types (Rasio & Shapiro 1995, Tylenda et al. 2011, Zhu et al. 2016). However, the question of when the CE phase leads to the ejection of the envelope (and a tighter binary) and when to a star merger remains without answer. Hence, this short-lived phase is one of the most important unsolved problems in stellar evolution.

Developing a binary evolutionary model requires knowing the fundamental parameters of the components stars. W UMa binaries, especially those that undergo total eclipses, are the most important sources of such information. Moreover, the study of deep-contact binaries may throw light on the fate of all types of binaries.

This work presents photometric observations and light curve solutions of six deep-contact W UMa binaries: V0637 Peg (ASAS 222153+2802.8; GSC 02226-02148; UCAC4 591-134612; 2MASS J22215338+2802471), V0473 Cam (GSC 04530-01042; 2MASS J07170493+7710260; UCAC4 836-008955), CSS J153314.8+560527 (2MASS J15331471+5605280; UCAC4 731-053285; GSC 03872-00076, and CSS J153314), CSS J075258.0+382035 (UCAC4 642-042673, 2MASS J07513566+3820286, and CSS J075258), V0416 Gem (GSC 01356-02826; ASAS J065947+2229.9) and NSVS 6859986 (GSC 02397-00333; 2MASS J05114146+3531357; UCAC4 628-022051). Table 1 shows the coordinates of our observation targets and the information available on their light variability.

2. OBSERVATIONS

The CCD photometric observations of the observation targets in the Sloan g', i' filters were performed at the Rozhen Observatory using the 30-cm Ritchey Chretien Astrograph (located in the *IRIDA South* dome) with an ATIK 4000 M CCD camera (2048 × 2048 pixels, 7.4μm/pixel, field of view 35 × 35 arcmin). Table 2 shows information of our observations.

The data were obtained during photometric nights with seeing in the range of 1.1–1.9 arcsec. The airmass of the observations of all targets was within the range 1.01–2.01. Twilight flat fields were obtained through each filter, as well as dark and bias frames. The frames were combined into a single master bias, and dark and flat frames. The reduction of the photometric data was done using the standard procedure (de-biasing, dark-frame subtraction and flat-fielding) with the software AIP4WIN v.2.0 (Berry & Burnell 2006).

For the stellar images, we used aperture photometry with a radius of 1.5 FWHM as well as sky background measurements in an annulus encompassing a comparable area. The light variability of the observation targets was estimated by comparing it with nearby (constant) stars in the observed field of each target (ensemble photometry). A check star served to determine the observational accuracy and to verify the constancy of the comparison stars. CCD ensemble photometry calculates the difference between the instrumental magnitude of the target and a comparison magnitude obtained from the mean of the intensities of the chosen comparison stars. The use of numerous comparison stars increases considerably the statistical accuracy of the comparison magnitude (Gilliland & Brown 1988, Honeycutt 1992).

We performed the ensemble aperture photometry with the software VPHOT (https://www.aavso.org/vphot). Table 3 shows the coordinates of the comparison and check stars, taken from the UCAC4 catalogue (Zacharias et al. 2013); their magnitudes were taken from the APASS DR9 catalogue (Henden et al. 2016).

According to the VSX database, the stars CSS J153314.8+560527 and NSVS 2808700 are very close in position and have almost equal periods. Our observations revealed that the second star is not variable.

The transformation of the instrumental magnitudes into standard ones was done manually. For this, we used the mean color of the ensemble comparison star $\overline{(g'-i')}_{comp}$ and the transformation coefficients of our equipment (Kjurkchieva et al. 2017).

Tables 8–13 in the Appendix show the templates derived from our photometric data (full tables are available at the CDS, $/CatS/217.174.158.82 : 004$.)

3. LIGHT CURVE SOLUTIONS

The IRIDA light curves of the observation targets were solved using the PHOEBE code (Prsa & Zwitter, 2005), which is based on the Wilson–Devinney (WD) code (Wilson & Devinney 1971, Wilson 1979, 1993) but has some improvements such as a graphical user interface and updates such as the Sloan filters used in our observations.

The target temperatures T_m were determined (Table 5) from their infrared color indices *(J-K)*, taken from the 2MASS catalog, and the color-temperature calibration of Tokunaga (2000).

TABLE 1

PARAMETERS OF OUR OBSERVATION TARGETS TAKEN FROM THE VSX DATABASE

Target	RA	Dec	Period [d]	mag	Ampl [mag]	Type
V0637 Peg	22 21 53.40	+28 02 47.0	0.311791	12.45(CV)	0.77	EW
V0473 Cam	07 17 04.93	+77 10 26.1	0.298438	11.55(R1)	0.65	EW
CSS J153314	15 33 14.71	+56 05 28.2	0.264594	12.81(CV)	0.47	EW
CSS J075258	07 52 58.09	+38 20 35.3	0.429914	13.07(CV)	0.37	EW
V0416 Gem	06 59 47.31	+22 29 48.6	0.256250	12.70(V)	0.50	EW
NSVS 6859986	05 11 40.85	+35 31 33.2	0.38356914	12.40(R1)	0.68	EW

TABLE 2

LOG OF OUR PHOTOMETRIC OBSERVATIONS

Target	Date	Exposure (g', i') [sec]	Number (g', i')	Error (g', i') [mag]
V0637 Peg	2016 Sep 22	120, 120	62, 62	0.006, 0.008
	2016 Sep 23	120, 120	79, 78	0.004, 0.006
	2016 Sep 24	120, 120	101, 99	0.006, 0.009
V0473 Cam	2015 Jan 1	60, 90	120, 120	0.003, 0.003
	2015 Jan 3	60, 90	39, 38	0.006, 0.006
CSS J153314	2016 Jun 20	120, 120	69, 68	0.007, 0.009
	2016 Jun 21	120, 120	62, 62	0.006, 0.008
CSS J075258	2016 Feb 9	180, 240	38, 39	0.003, 0.006
	2016 Feb 15	180, 240	63, 62	0.004, 0.006
	2016 Feb 28	180, 240	35, 34	0.004, 0.007
	2016 Mar 6	180, 240	36, 34	0.003, 0.006
	2016 Feb 17	180, 240	48, 48	0.004, 0.006
	2016 Feb 18	180, 240	59, 58	0.006, 0.008
V0416 Gem	2016 Dec 3	60, 90	48, 48	0.010, 0.013
	2016 Dec 4	60, 90	85, 85	0.005, 0.006
	2016 Dec 5	60, 90	125, 125	0.005, 0.006
	2016 Dec 6	60, 90	31, 31	0.005, 0.006
	2016 Dec 8	60, 90	32, 32	0.005, 0.007
	2016 Dec 9	60, 90	87, 87	0.005, 0.007
	2016 Dec 10	60, 90	165, 165	0.005, 0.007
NSVS 6859986	2016 Nov 24	60, 90	132, 132	0.004, 0.005
	2016 Nov 25	60, 90	91, 91	0.004, 0.006
	2016 Nov 27	60, 90	139, 139	0.009, 0.011

The initial runs revealed that all observation targets are overcontact systems. Thus, we used the "Overcontact Binary not in Thermal Contact" mode of the code. The fit quality was estimated based on the value χ^2.

First, we fixed $T_1 = T_m$ and varied the initial epoch T_0 and period P to fit the light curves to the phases of light minima and maxima. Afterwards, we fixed T_0 and P, and varied simultaneously the secondary temperature T_2, the orbital inclination i, the

TABLE 3

LIST OF THE STANDARD STARS

Label	Star ID	RA	Dec	g'	i'
Target	V0637 Peg	22 21 53.40	+28 02 47.00	13.24	12.24
Chk	UCAC4 591-134602	22 21 47.14	+28 05 28.21	14.360	13.201
C1	UCAC4 590-134319	22 21 58.53	+27 57 39.13	13.700	13.190
C2	UCAC4 590-134268	22 21 27.93	+27 58 29.23	14.206	13.301
C3	UCAC4 590-134302	22 21 48.22	+27 59 26.26	13.982	13.359
C4	UCAC4 591-134550	22 21 15.51	+28 04 13.34	13.539	12.884
C5	UCAC4 591-134590	22 21 38.84	+28 05 26.42	13.229	12.297
C6	UCAC4 591-134573	22 21 31.08	+28 07 20.65	13.213	12.615
C7	UCAC4 591-134594	22 21 41.55	+28 08 12.48	13.318	12.713
C8	UCAC4 591-134609	22 21 51.23	+28 08 03.18	13.773	13.106
C9	UCAC4 591-134625	22 21 59.90	+28 05 28.35	13.329	12.661
C10	UCAC4 590-134318	22 21 57.52	+27 55 26.19	13.479	12.254
Target	V0473 Cam	07 17 04.93	+77 10 26.10	11.860	11.101
Chk	UCAC4-837-008887	07 17 11.21	+77 12 38.47	12.231	11.248
C1	UCAC4-837-008919	07 19 47.76	+77 17 47.18	12.650	12.049
C2	UCAC4-837-008907	07 18 47.34	+77 18 04.02	12.386	11.084
C3	UCAC4-837-008861	07 15 04.93	+77 17 40.46	12.664	11.738
C4	UCAC4-837-008897	07 18 12.24	+77 15 46.18	13.047	11.812
C5	UCAC4-836-008980	07 19 10.50	+77 10 27.41	13.049	12.201
C6	UCAC4-836-008968	07 18 01.77	+77 11 57.23	12.428	11.966
C7	UCAC4-836-008948	07 16 26.49	+77 05 33.45	13.243	12.059
C8	UCAC4-836-008929	07 15 08.62	+77 09 09.54	12.003	11.303
Target	CSS J153314	15 33 14.71	+56 05 28.25	12.981	12.076
Chk	UCAC4 731-053305	15 34 24.40	+56 04 59.16	14.041	12.736
C1	UCAC4 731-053289	15 33 23.47	+56 05 26.31	12.567	11.645
C2	UCAC4 731-053282	15 33 03.52	+56 07 03.97	13.202	12.249
C3	UCAC4 731-053294	15 33 38.81	+56 10 18.03	12.473	11.881
C4	UCAC4 731-053302	15 34 05.08	+56 02 54.73	12.803	12.067
C5	UCAC4 730-053151	15 33 43.32	+55 59 24.05	12.976	12.507
C6	UCAC4 730-053123	15 32 23.54	+55 56 07.04	11.544	11.043
C7	UCAC4 732-053671	15 33 00.50	+56 15 00.72	10.806	9.762
Target	CSS J075258	07 52 58.09	+38 20 35.30	13.205	12.746
Chk	UCAC4 643-044185	07 51 20.51	+38 34 24.58	14.121	13.686
C1	UCAC4 643-044208	07 51 47.59	+38 35 55.44	14.120	13.657
C2	UCAC4 643-044212	07 51 49.87	+38 35 24.70	14.660	13.681
C3	UCAC4 643-044217	07 51 54.27	+38 32 17.07	14.572	13.818
C4	UCAC4 643-044225	07 52 03.85	+38 32 23.81	14.709	14.018
C5	UCAC4 643-044233	07 52 15.03	+38 31 48.84	13.911	13.311
C6	UCAC4 643-044248	07 52 40.64	+38 32 08.27	14.134	13.686
C7	UCAC4 643-044271	07 53 09.97	+38 31 21.83	13.671	13.366
C8	UCAC4 643-044218	07 51 54.46	+38 29 44.02	14.346	13.859

TABLE 3 (CONTINUED)

Label	Star ID	RA	Dec	g'	i'
C9	UCAC4 643-044228	07 52 07.68	+38 27 03.01	13.635	13.310
C10	UCAC4 643-044235	07 52 19.56	+38 25 59.02	14.447	13.755
C11	UCAC4 643-044258	07 52 55.66	+38 24 46.13	14.096	13.712
C12	UCAC4 642-042689	07 52 04.30	+38 21 25.15	14.479	13.864
Target	V0416 Gem	06 59 47.30	+22 29 48.60	13.052	12.312
Chk	UCAC4 563-036983	06 59 49.78	+22 28 44.10	13.996	13.107
C1	UCAC4 563-036939	06 59 31.19	+22 24 51.76	13.434	12.208
C2	UCAC4 564-035265	06 59 56.51	+22 38 18.59	12.759	12.403
C3	UCAC4 564-035241	06 59 46.10	+22 37 57.21	13.819	12.233
C4	UCAC4 563-037084	07 00 22.57	+22 34 21.09	11.846	11.622
C5	UCAC4 562-037143	06 59 33.94	+22 23 58.71	12.137	11.927
C6	UCAC4 563-036842	06 58 58.09	+22 35 54.85	12.787	11.816
Target	NSVS 6859986	05 11 40.85	+35 31 33.20	12.768	11.795
Chk	UCAC4 628-022093	05 11 58.38	+35 28 58.92	13.038	11.868
C1	UCAC4 628-022028	05 11 34.61	+35 31 11.10	13.404	11.825
C2	UCAC4 628-022102	05 12 01.20	+35 30 34.47	13.312	12.240
C3	UCAC4 628-022047	05 11 40.82	+35 35 56.50	13.583	12.860
C4	UCAC4 628-021932	05 11 05.18	+35 30 09.89	13.791	11.350
C5	UCAC4 629-021294	05 11 19.47	+35 38 16.99	13.402	12.517
C6	UCAC4 629-021303	05 11 21.82	+35 37 42.51	14.105	13.456
C7	UCAC4 628-022146	05 12 12.73	+35 35 42.36	13.770	12.774
C8	UCAC4 628-022184	05 12 25.68	+35 31 48.49	13.408	11.849
C9	UCAC4 628-022229	05 12 39.46	+35 32 05.42	14.106	12.259

TABLE 4

VALUES OF THE FITTED PARAMETERS

Star	T_0	Ω	q	i	T_2
V0637 Peg	2457372.21954(5)	2.73(3)	0.501(1)	88(4)	4587(32)
V0473 Cam	2457024.41640(3)	2.66(2)	0.47(3)	84.7(8)	5100(41)
CSS J153314	2457560.42347(7)	5.7(3)	2.6(2)	86(1)	4933(567)
CSS J075258	2457434.43750(8)	9.5(2)	5.6(1)	84.3(6)	6070(23)
V0416 Gem	2457726.45333(9)	10.8(2)	6.7(2)	73.2(7)	5420(294)
NSVS 6859986	2457718.50448(9)	8.3(3)	4.8(3)	89(1)	5100(680)

mass ratio q and the potential Ω to try to reproduce complete light curves.The data in the i' and g' bands were modelled simultaneously.

We used gravity brightening coefficients of $g_1 = g_2 = 0.32$ and reflection effect coefficients of $A_1 = A_2 = 0.5$, which are appropriate for late-type stars; the linear limb-darkening coefficients for each component and each color were updated according to the tables of Van Hamme (1993). Solar metallicity was assumed for the targets because they consist of late stars from the solar vicinity.

In order to reproduce the light curve anomalies, we used cool spots. Varying the parameters of these spots (longitude λ, angular size α and temperature factor κ) simultaneously with the other configuration parameters often led to non-physical values. This is why the spot parameters were adjusted "manually" (within reasonable ranges). Due to the ambiguous-

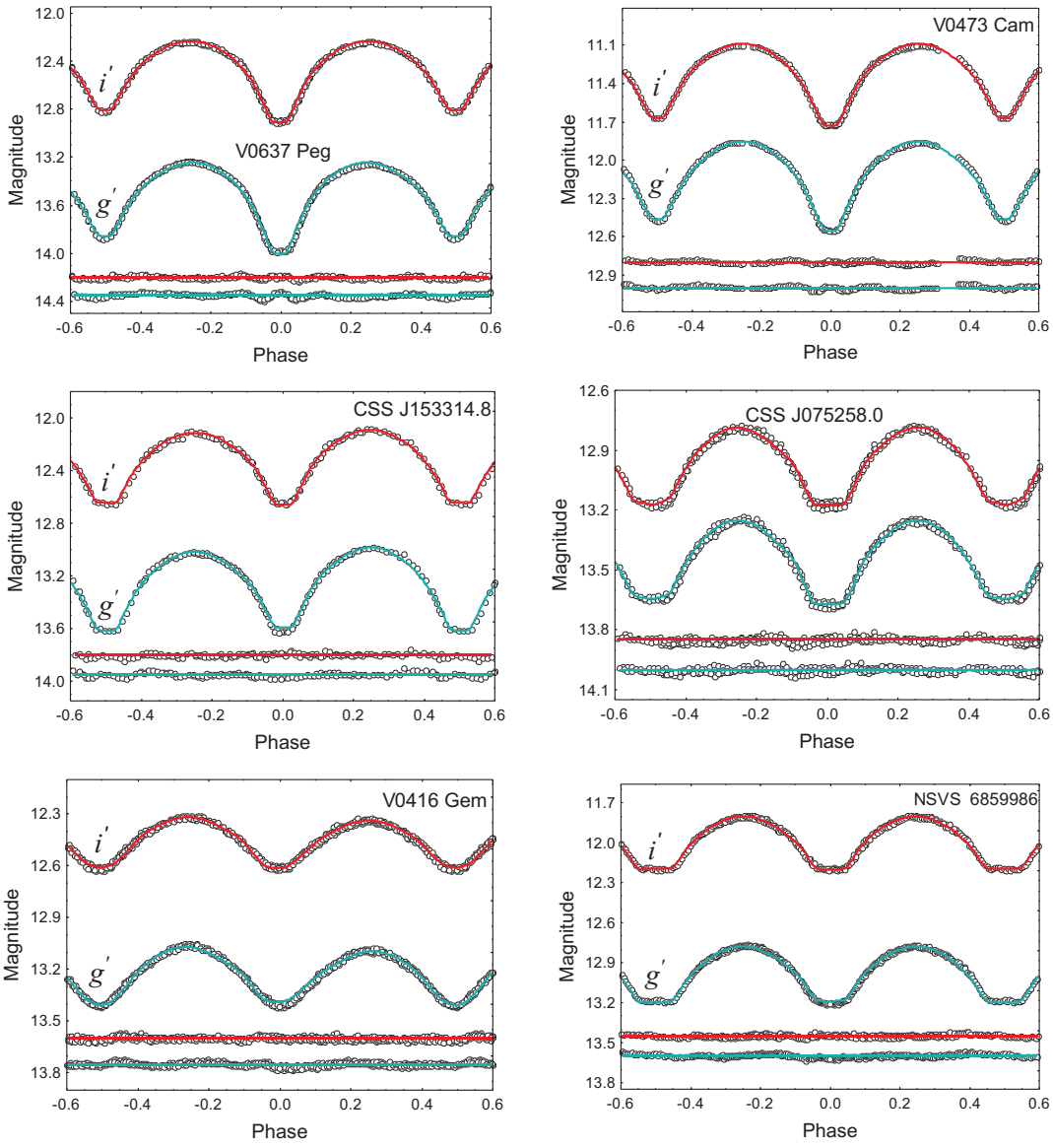

Fig. 1. The folded light curves of the observation targets with their fits and residuals (shifted vertically by different amounts to save space).

TABLE 5

CALCULATED PARAMETERS

Star	T_m	T_1^f	T_2^f	r_1	r_2	f	l_2/l_1
V0637 Peg	4903	4997(50)	4681(40)	0.479(1)	0.361(1)	0.504	0.429
V0473 Cam	5300	5361(50)	5161(60)	0.487(1)	0.357(1)	0.539	0.459
CSS J153314	4933	4933(567)	4933(567)	0.340(1)	0.504(2)	0.566	2.268
CSS J075258	6203	6227(60)	6094(50)	0.273(1)	0.560(2)	0.630	3.851
V0416 Gem	5420	5420(294)	5420(294)	0.259(1)	0.573(2)	0.651	5.058
NSVS 6859986	5100	5100(616)	5100(616)	0.302(1)	0.560(2)	0.864	3.756

ness of the solution of the inverse problem, we chose almost equatorial spots on the primary stars because they have the smallest size and temperature contrast required to fit a given light curve distortion.

After finding the best solution we varied all parameters together (T_2, i, q, Ω, T_0 and P) around the values from the last run and obtained the final model.

In order to adjust the stellar temperatures T_1^f and T_2^f, around the value T_m, we used the following formulae (Ivanov et al. 2010):

$$T_1^f = T_m + c\frac{\Delta T}{c+1}, \quad (1)$$

$$T_2^f = T_1 - \Delta T, \quad (2)$$

where $c = l_2/l_1$ (luminosity ratio) and $\Delta T = T_m - T_2$ were taken from the final PHOEBE fit.

Although PHOEBE (as well as WD) works with potentials, it allows to calculate directly the values (polar, point, side, and back) of the relative radius $r_i = R_i/a$ of each component (R_i is the linear radius and a is orbital separation). In the absence of radial velocity curves, we chose as default $a = 1$. Moreover, PHOEBE yields the bolometric magnitudes M^i_{bol} of the two component stars in conditional units (when radial velocity data are not available). Their difference $M^2_{bol} - M^1_{bol}$ determines the true luminosity ratio $c = L_2/L_1 = l_2/l_1$. The fill-out factor $f = [\Omega - \Omega(L_1)]/[\Omega(L_2) - \Omega(L_1)]$ can also be calculated from the output parameters of the PHOEBE solution.

Table 4 shows the final values of the fitted stellar parameters and their uncertainties: initial epoch T_0; mass ratio q; inclination i; potential Ω; secondary temperature T_2. The mass ratios correspond to the ratio between the mass of the primary component and the mass of the star eclipsed at MinI. The orbital periods P from Table 1 fitted our data well.

Table 5 shows the following calculated parameters: stellar temperatures $T^f_{1,2}$; stellar radii $r_{1,2}$ (back values); fill-out factor f; stellar luminosity ratio l_2/l_1. Their errors are determined from the uncertainties of the output parameters used for the calculation. Table 6 shows information on the spot parameters and their uncertainties.

The synthetic light curves corresponding to our solutions are shown in Figure 1 as continuous lines. At most phases, the residuals do not affect the observational precision (see Table 1) but they are larger during the eclipses of some targets (especially the primary eclipses of V0637 Peg and V0473 Cam). Attempts to improve the fits by introducing nonlinear limb-darkening laws (logarithmic and square root) and arbitrarily varying the limb-darkening coefficients arbitrary were unsuccessful. We suspect that the reason for this are numerical imprecisions in the physical model of deep-contact binaries. It should be pointed out that this behavior of the residual curves can be observed even in some *Kepler* binaries (Hambleton et al. 2013, Lehmann et al. 2013, Maceroni et al. 2014). Kipping (2010) attributed it to the effects of finite integration time, while Prsa et al. (2016) attributed it to an inadequate treatment of overcontact binaries, especially of their neck regions.

The main results of our model are as follows: (i) All observation targets undergo total eclipses, which means that their photometric mass ratios can be determined with great confidence (Terrell & Wilson 2005); (ii) the components of each target are almost equal in temperature and are of the G and K spectral types (Table 5); (iii) All targets have deep-contact

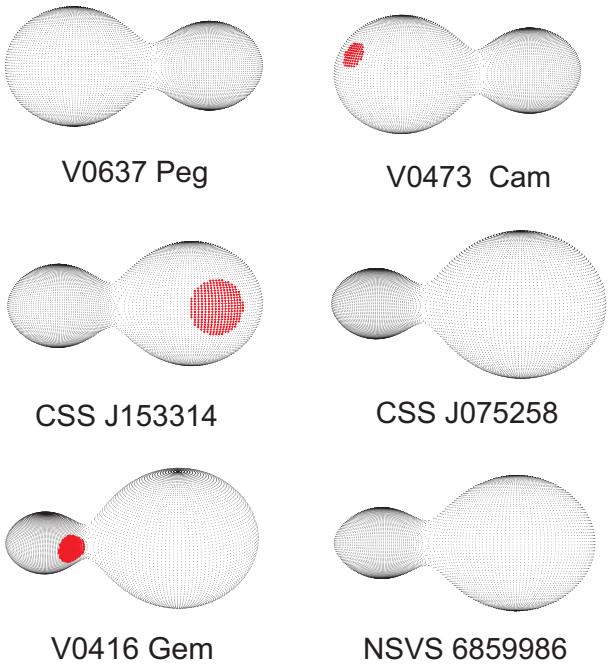

Fig. 2. 3D configurations of the targets.

TABLE 6

PARAMETERS OF THE SURFACE SPOTS

star	β [°]	λ [°]	α [°]	k
V0473 Cam	70(5)	200(2)	12(0.5)	1.1(0.1)
CSS J153314	90(5)	100(2)	25(1)	0.9(0.1)
V0416 Gem	90(5)	310(2)	24(1)	0.8(0.1)

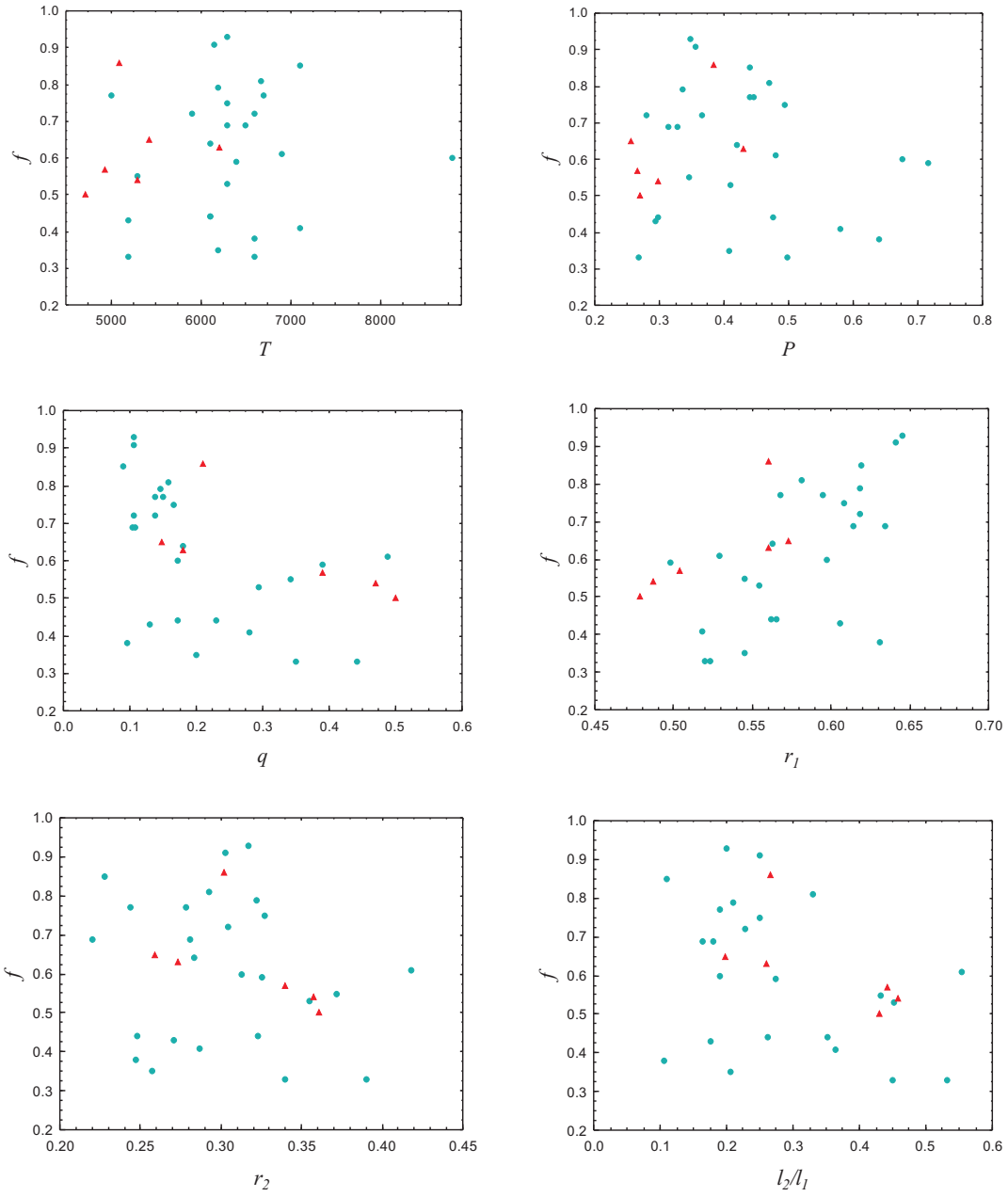

Fig. 3. Empirical relationships between the fill-out factor and stellar parameters (the red triangles indicate our targets; the blue circles indicate for other overcontact systems from Table 7). The color figure can be viewed online.

configurations (Figure 2, Table 5) with a fill-out factor $f > 0.5$ that reaches $f = 0.84$ for NSVS 6859986; (iv) The values of $l_2/l_1, q, r_2/r_1$ shown in Tables 4–5 confirm the assumption that the luminosity ratio for deep-contact binaries (whose components have equal temperatures) depends on the squared ratio of the components' radii but not on the mass ratio. This means that the empirical relation between the global parameters of deep-contact binaries are different from those of MS stars.

4. DEEP-CONTACT BINARIES

In order to study the dependencies between the fill-out factor and the stellar parameters of deep-contact systems, as well as to verify if they corre-

TABLE 7

PARAMETERS OF DEEP-CONTACT BINARIES SORTED BY INCREASING FILLOUT FACTOR

star	T_m	P	q	Ω	r_1	r_2	f	l_2/l_1	Ref
DN Cam	6600	0.498	0.442	5.319	0.523	0.39	0.33	0.53	1
EK Com	5200	0.267	0.35	2.501	0.523	0.344	0.33	0.449	2
EX Leo	6200	0.408	0.2	2.186	0.545	0.257	0.35	0.206	3
FP Boo	6600	0.640	0.096	1.922	0.631	0.247	0.38	0.105	4
BX Dra	7100	0.579	0.28	2.351	0.518	0.287	0.41	0.363	3
V902 Sgr	5200	0.294	0.13	2.019	0.606	0.271	0.43	0.176	5
AQ Psc	6100	0.476	0.231	2.244	0.565	0.323	0.44	0.352	4
OU Ser	6100	0.297	0.172	2.113	0.562	0.248	0.44	0.263	6
V1918 Cyg	7000	0.413	0.264	2.303	0.559	0.340	0.49	0.298	7
V0637 Peg	4903	0.311	0.50	2.727	0.479	0.361	0.50	0.429	8
V839 Oph	6300	0.409	0.294	2.357	0.554	0.355	0.53	0.453	4
V0473 Cam	5300	0.298	0.47	2.659	0.487	0.357	0.54	0.459	8
ET Leo	5300	0.346	0.342	6.178	0.545	0.372	0.55	0.432	4
CSS J153314	4933	0.265	0.39	5.71	0.504	0.340	0.57	0.441	8
V592 Per	6400	0.716	0.389	2.526	0.498	0.325	0.59	0.275	6
IK Per	8800	0.676	0.171	2.094	0.597	0.313	0.60	0.19	9
NN Vir	6900	0.481	0.487	2.674	0.529	0.418	0.61	0.555	10
CSS J075258	6203	0.430	0.18	9.54	0.560	0.273	0.63	0.26	8
Y Sex	6100	0.420	0.18		0.563	0.283	0.64		11
V0416 Gem	5420	0.256	0.148	10.84	0.573	0.259	0.65	0.198	8
V1191 Cyg	6500	0.313	0.107	1.933	0.634	0.281	0.69	0.163	12
FG Hya	6300	0.328	0.104	1.924	0.614	0.22	0.69	0.179	3
ASAS J082243	6600	0.28008	0.106				0.72		13
V410 Aur	5900	0.366	0.137	2.004	0.618	0.304	0.72	0.227	4
AH Aur	6300	0.494	0.165	2.064	0.608	0.327	0.75	0.25	10
V776 Cas	6700	0.440	0.138	2.001	0.595	0.244	0.77	0.19	6
TV Mus	5900	0.446	0.15		0.568	0.278	0.77		14, 15
DZ Psc	6200	0.366	0.145	2.015	0.618	0.322	0.79	0.21	10
V728 Her	6670	0.471	0.158	2.024	0.581	0.293	0.81	0.33	16
AW UMa	7100	0.439	0.09		0.619	0.228	0.85	0.11	17, 18
NSVS 6859986	5100	0.383	0.209	8.33	0.560	0.302	0.86	0.26	8
CK Boo	6150	0.355	0.106	1.915	0.641	0.303	0.91	0.25	4
GR Vir	6300	0.347	0.106	1.913	0.645	0.317	0.93	0.20	10

References: 1- Baran et al. 2004; 2 - Deb et al. 2010; 3 - Zola et al. 2010; 4 - Gazeas et al. 2006; 5 - Samec & Corbin 2002; 6 - Zola et al. 2005; 7 - Yang et al. 2013; 8 - this paper; 9 - Zhu et al. 2005; 10 - Gazeas et al. 2005; 11 - Yang & Liu 2003; 12 - Zhu et al. 2011; 13 - Kandulapati et al. 2015; 14 - Maceroni & van't Veer 1996; 15 - Qian et al. 2005; 16 - Erkan & Ulas 2016; 17 - Yang 2008; 18 - Rucinski 2015.

spond to theoretical predictions, we performed a statistical analysis of our targets and several tens of well studied overcontact systems (Table 7). For targets with $q > 1$, we changed the order of the components, which means that: (i) the mass ratios were substituted by their inverse values; (ii) the luminosity ratios were substituted by their inverse values; (iii) the relative radii and temperatures of the stellar

components were exchanged for each other. For targets with more than one solution, we used the newest one (e.g. FG Hya).

The diagrams of the relationships between the fill-out factor and the -configuration parameters (Figure 3) show rather scattered distributions that cannot be fitted to any function. However, we were able to identify some qualitative tendencies.

(1) The fill-out factor f seems not to depend on stellar temperature.

(2) A tendency of f to increase with decreasing periods P corresponds to theoretical predictions. But there are deviations from this tendency; for instance, EK Com has a period of 0.27 days and f=0.33.

(3) The fill-out factor increases as the mass ratio decreases, in agreement with theoretical predictions. But there are deviations from this tendency; for instance, FP Boo has $q \approx 0.1$ and a moderate fill-out factor of 0.38 (Figure 3).

(4) We found a tendency for f to increase as the primary radius r_1 increases.

(5) The fill-out factor tends to increase as the secondary radius r_2 decreases, and also as the luminosity ratio l_2/l_1 decreases (Figure 3).

These tendencies are in agreement with the expected physically relationships, but there are deviations from them, especially for moderate values of f (Figure 3).

This analysis leads to the question of which of the targets shown Figure 3 will become progenitors of tight binaries and which will merge. Or is there another evolutionary outcome?

5. CONCLUSION

Our observations and light curve solutions showed that V0637 Peg, V0473 Cam, CSS J153314, CSS J075258, V0416 Gem and NSVS 6859986 have deeply overcontact configurations with fill-out factors above 0.5. The components of all the observation targets have almost equal temperatures and undergo total eclipses.

We studied the dependencies between the fill-out factor and stellar parameters (temperature, period, relative stellar radii, mass ratio, luminosity ratio) in a sample of three dozens deep-contact binaries. Most of them are consistent with theoretical predictions of the evolutionary scenarios but there are deviations from the common tendencies.

This study adds estimated parameters for six new deep-contact systems to the family of W UMa binaries. The statistical analysis of the dependencies between the fill-out factor and the stellar parameters of deep-contact systems opens new questions about the evolutionary fate of such configurations.

This work was supported partly by project HD08/20 of the Foundation for Scientific Research of the Bulgarian Ministry of Education and Science as well as by project RD 08-102 of Shumen University. This publication makes use of data products from the Two Micron All Sky Survey, which is a joint project of the University of Massachusetts and the Infrared Processing and Analysis Center/California Institute of Technology, funded by the National Aeronautics and Space Administration and the National Science Foundation. This research also makes use of the SIMBAD database, operated at CDS, Strasbourg, France, the NASA Astrophysics Data System Abstract Service, the USNOFS Image and Catalogue Archive operated by the United States Naval Observatory, the Flagstaff Station (http://www.nofs.navy.mil/data/fchpix/) and the photometric software VPHOT operated by the AAVSO, Cambridge, Massachusetts (https://www.aavso.org/vphot). The authors are very grateful to the anonymous referee for the valuable suggestions and notes.

APPENDIX

A. TABLES WITH PHOTOMETRIC DATA

TABLE 8

PHOTOMETRIC DATA OF V0637 PEG

HJD	mag	Error	Filter
2457654.23887871	13.843	0.006	g'
2457654.24208867	13.801	0.005	g'
2457654.24542862	13.750	0.005	g'
...	...	...	...
2457654.24047869	12.769	0.007	i'
2457654.24380864	12.732	0.007	i'
2457654.24714859	12.683	0.007	i'
...	...	...	...

TABLE 9

PHOTOMETRIC DATA OF V0473 CAM

HJD	mag	Error	Filter
2457024.227290	11.971	0.003	g'
2457024.229490	11.987	0.003	g'
2457024.231690	12.008	0.003	g'
...	...	...	...
2457024.228380	11.199	0.003	i'
2457024.230590	11.216	0.003	i'
2457024.232790	11.240	0.003	i'
...	...	...	...

TABLE 10

PHOTOMETRIC DATA OF CSS J153314

HJD	mag	Error	Filter
2457560.317616	13.245	0.007	g'
2457560.320796	13.213	0.007	g'
2457560.323946	13.165	0.007	g'
...	...	...	...
2457560.319226	12.318	0.009	i'
2457560.322376	12.285	0.009	i'
2457560.325526	12.250	0.009	i'
...	...	...	...

TABLE 11

PHOTOMETRIC DATA OF CSS J075258

HJD	mag	Error	Filter
2457428.219764	13.653	0.003	g'
2457428.225044	13.646	0.003	g'
2457428.230404	13.616	0.003	g'
...	...	...	...
2457428.217135	13.186	0.006	i'
2457428.222394	13.177	0.006	i'
2457428.227684	13.168	0.006	i'
...	...	...	...

TABLE 12

PHOTOMETRIC DATA OF V0416 GEM

HJD	mag	Error	Filter
2457726.36569356	13.124	0.005	g'
2457726.36781367	13.111	0.005	g'
2457726.36996379	13.108	0.005	g'
...	...	...	...
2457726.36674362	12.366	0.006	i'
2457726.36887373	12.348	0.006	i'
2457726.37102385	12.356	0.008	i'
...	...	...	...

TABLE 13

PHOTOMETRIC DATA OF NSVS 6859986

HJD	mag	Error	Filter
2457717.38869749	13.006	0.004	g'
2457717.39084756	12.991	0.004	g'
2457717.39301762	12.969	0.004	g'
...	...	...	...
2457717.38976753	12.019	0.006	i'
2457717.39193759	12.014	0.006	i'
2457717.39408765	11.978	0.005	i'
...	...	...	...

REFERENCES

Baran, A., et al. 2004, AcA, 54, 195
Berry, R. & Burnell, J. 2006, The Handbook of Astronomical Image Processing with AIP4WIN2 software, Willmannn-Bell.Inc., WEB
Binnendijk, L. 1965, VeBam, 27, 36
Deb, S., et al. 2010, NewA, 15, 662
Eker, Z., Bilir, S., Yaz, E., Demircan, O., & Helvaci, M. 2008, AN, 999, 157
Erkan, N. & Ulas, B. 2016, NewA, 46, 73
Gazeas, K., et al. 2005, AcA, 55, 123
Gazeas, K., et al. 2006, AcA, 56, 127
Gettel, S. J., Geske, M. T., & McKay, T. A. 2006, AJ, 131, 621
Gilliland, R. & Brown, T. 1988, PASP, 100, 754
Hambleton, K., et al. 2013, MNRAS, 434, 925
Henden, A. 2016, JAVSO, 44, 84
Honeycutt, R. K. 1992, PASP, 104, 435
Ivanov, V. P. & Kjurkchieva, D. P. 2010, BASI, 38, 83
Ivanova, N., et al. 2013, A&ARv, 21, 59
Kandulapati, S., Devarapalli, S. P., & Pasagada, V. R. 2015, MNRAS, 446, 510
Kipping, M., 2010, MNRAS, 408, 1758
Kjurkchieva, D., Popov, V., Vasileva, D., & Petrov, N. 2017, RMxAA, 53, 133
Klagyivik, P. & Csizmadia, Sz. 2004, PADEU, 14, 303
Lehmann, H., et al. 2013, A&A, 557A, 79
Lucy, L. B. 1968a, ApJ, 151, 1123
_____. 1968b, ApJ, 153, 877
Maceroni, C., & van't Veer, F. 1996, A&A, 311, 523
Maceroni, C., et al. 2014, A&A, 563A, 59

Martin, E. L., Spruit, H. C., & Tata, R. 2011, A&A, 535, A50
Munari, U., Henden, A., Kiyota, S., et al. 2002, A&A, 389, L51
Prsa, A. & Zwitter, T. 2005, ApJS, 628, 426
Prsa, A., et al. 2016, ApJS, 227, 29
Qian, S.-B. 2003, MNRAS, 342, 1260
Qian, S. & Yang, Y. 2005, MNRAS, 356, 765
Qian, S.-B., Yang, Y.-G., Soonthornthum, B., et al. 2005, AJ, 130, 224
Qian, S.-B., Liu, L., Zhu, L.-Y., et al. 2011, AJ, 141, 151
Rasio, F. & Shapiro, S. 1995, ApJ, 438, 887
Rucinski, S. M. 2015, AJ, 149, 49
Samec, R. & Corbin, S. 2002, IBVS, 5259, 1
Stepien, K. 2006, AcA, 56, 199
Terrell, D. & Wilson, R. 2005, ApSpSci, 296, 221
Tokunaga, A. T. 2000, Allen's astrophysical quantities, Edited by Arthur N. Cox, New York: AIP Press; Springer
Tylenda, R., et al. 2011, A&A, 528A, 114
Van Hamme, W. 1993, AJ, 106, 2096
Webbink, R. F. 1984, ApJ, 277, 355
Willems, B. & Kolb, U. 2004, A&A, 419, 1057
Wilson, R. 1979, ApJ, 234, 1054
_____. 1993, ASPC, 38, 91
Wilson, R. & Devinney, E. 1971, ApJ, 166, 605
Yang, Y. 2008, Ap&SS, 314, 151
Yang, Y.-G., Qian, S.-B., Zhang, L.-Y., Dai, H.-F., & Soonthornthum, B. 2013, AJ, 146, 35
Yang, Y.-L. & Liu, Q.-Y. 2003, NewA, 8, 465
Zacharias, N., et al. 2013, AJ, 145, 44
Zola, S., et al. 2005, Acta Astron., 55, 389
Zola, S., et al. 2010, MNRAS, 408, 464
Zhu, L., Qian, S.-B., Soonthornthum, B., & Yang, Y.-G. 2005, AJ, 129, 2806
Zhu, L. Y., Qian, S. B., Soonthornthum, B., He, J. J., & Liu, L. 2011, AJ, 142, 124
Zhu, L., Zhao, E., & Zhou, X. 2016, RAA, 16, 68

D. Kjurkchieva and D. Vasileva: Department of Physics, Shumen University, 9700 Shumen, Bulgaria (d.kyurkchieva, d.vasileva@shu.bg).
V. A. Popov: IRIDA Observatory, Rozhen NAO, Bulgaria (velimir.popov@elateobservatory.com).
N. Petrov: Institute of Astronomy and NAO, Bulgarian Academy of Sciences, Tsarigradsko shossee 72, 1784 Sofia, Bulgaria (nip.sob@gmail.com).